**Title:** HIV-1 accessory protein Vpr interacts with REAF and mitigates its associated antiviral activity.

**Short title:** Vpr mitigates REAF

**Authors:** Joseph M Gibbons[1], Kelly M Marno[1], Rebecca Pike[1], Wing-yiu Jason Lee[1], Christopher E Jones[1], Babatunji W Ogunkolade[1], Claire Pardieu[1], Alexander Bryan[2], Rebecca Menhua Fu[2], Gary Warnes[1], Paul A Rowley[3], Richard D Sloan[2,4] and Áine McKnight[1]

## Abstract

The accessory protein Vpr of Human Immunodeficiency Virus type 1 (HIV-1) enhances replication of the virus in macrophage but less so in cycling T cells. Virus particle packaged Vpr is released in target cells shortly after entry, suggesting it is required early in infection. A commonly observed activity of Vpr is the induction of cell cycle arrest in T cells but why this is so is unknown. Here we observe, by co-immunoprecipitation assay, an interaction between Vpr and endogenous REAF (RNA-associated Early-stage Antiviral Factor, RPRD2), a protein previously shown to potently restrict HIV infection. After HIV-1 infects macrophages, within 30 minutes of viral entry, Vpr induces the degradation of REAF. Subsequently, as replication continues, REAF expression is upregulated – a response curtailed by Vpr. Using VLPs we show that Vpr alone is sufficient to down modulate REAF in MDMs. REAF is more highly expressed in differentiated macrophages than in cycling T cells. Expression in cycling cells is cell cycle dependent and knockdown induces cell cycle perturbation. Therefore, our results support the hypothesis that Vpr induces the degradation of a factor involved in the cell cycle that impedes HIV infection in macrophages.

[1]The Blizard Institute, Queen Mary University of London School of Medicine and Dentistry, QMUL, UK.
[2]Infection Medicine, The University of Edinburgh, UK.
[3] Department of Biological Sciences, The University of Idaho, Moscow, Idaho, USA.
[4]ZJU-UoE Institute, Zhejiang University, P.R. China.

# Introduction

Human Immunodeficiency Virus type 1 (HIV-1) infects $CD4^+$ T cells and macrophages *in vivo* and causes Acquired Immunodeficiency Syndrome (AIDS). HIV-1 has four non-structural accessory genes *nef, vif, vpu* and *vpr*. *Nef, vif and vpu* mitigate host innate immunity. A function for Vpr has been elusive, but it is required for replication in macrophages and for pathogenesis *in vivo* (1, 2). A widely acknowledged but poorly understood Vpr-mediated phenotype is that an infected population of cycling cells accumulates in the G2/M phase of the cell cycle. The observed phenomenon is achieved by manipulation of the cullin4A-DBB1 (DCAF1) E3 ubiquitin ligase and the recruitment of an unknown substrate for proteasomal degradation. A large number of Vpr substrates have been proposed (3-11). Yan *et al.* (2019) show that helicase-like transcription factor (HLTF) restricts replication of HIV-1 in T cells shown previously by Lahouassa *et al*. 2016 to be down modulated by Vpr about six hours post infection (12, 13). Furthermore, Greenwood *et al.* 2019 report on the effect that Vpr has on large scale remodelling of nearly 2000 cellular proteins including those that bind nucleic acids and those involved with the cell cycle (14).

Substantial but finite quantities of Vpr are incorporated into viral particles and released from the major capsid protein (CA) after entry into the cell (15, 16). Concurrently, reverse transcription transcribes the RNA genome into DNA, which integrates into the host cell DNA. The early release of Vpr from the CA (17) suggests it has an early function prior to integration. When considering the role of Vpr in cell tropism and pathogenesis it is important to focus on proteins that have a direct effect on viral replication. Here we show that within 30 minutes of cellular entry, Vpr containing virus induces the degradation of RNA-associated Early-stage Antiviral Factor (REAF, also known as RPRD2). REAF has been shown to limit the completion of pro-viral DNA

synthesis and integration (18). Here we show that it restricts replication of HIV-1 in macrophages, a restriction overcome by Vpr.

# Results

## HIV-1 Vpr interacts with REAF and overcomes restriction.

HeLa-CD4, knocked down for REAF (HeLa-CD4 shRNA-REAF, Figure 1A) were challenged with two HIV-1 primary macrophage tropic isolates 89.6 and 2044 (19). Figure 1B showns both viruses could replicate more efficiently in the absence of REAF (between 20 and 50 fold). To determine if a viral accessory gene could overcome this REAF effect we tested infectivity of HIV-1 $89.6^{WT}$ and mutants deleted for *vpr* ($89.6^{\Delta vpr}$), *vif* ($89.6^{\Delta vif}$) or *vpu* ($89.6^{\Delta vpu}$). Figure 1C shows that despite a standard virus input (50 FFU/ml, as measured on HeLa-CD4), the prevention of REAF expression using short hairpin RNA (shRNA) alleviates the need for Vpr. There is significantly greater rescue of HIV-1 $89.6^{\Delta vpr}$ (>40 fold, $p < 0.0001$) compared to HIV-1 $89.6^{WT}$ or other mutant viruses with an intact *vpr* gene but lacking *vpu* or *vif*. Thus, *vpr* potently overcomes the restriction imposed by REAF. We further confirmed that the mutant HIV-1 $89.6^{\Delta vpr}$ is restricted in HeLa-CD4 compared to HIV-1 $89.6^{WT}$. Figure 1D shows that despite equal inputs of p24, significantly fewer foci of infection (FFU) result from challenge with HIV-1 $89.6^{\Delta vpr}$ compared to HIV-1 $89.6^{WT}$. Further support of a role for Vpr is supported in Figures 1E and F. When PM1 cells are challenged with a HIV-1 $89.6^{WT}$, which has an intact *vpr*, REAF protein is down modulated (Figure 1E). The observed down modulation is dependent on the presence of Vpr as HIV-1 $89.6^{\Delta vpr}$ is incapable of degrading REAF (Figure 1F). Moreover, Figure 1G shows that Vpr and REAF interact with each other, either directly or as part of a complex, as they are co-immunoprecipitated.

Macrophages are a target for HIV infection (20) and numerous studies support the notion that *vpr* is crucial for their efficient infection. We therefore focussed on REAF effects in this primary cell type. Using Western blotting we followed REAF protein during the maturation of blood derived monocytes (day 0) to macrophages (Figure 3H). We observed that REAF levels increase over time up to 7 days of maturation. To investigate the ability of Vpr to deplete REAF protein in MDMs we used imaging flow cytometry to quantify the overall REAF mean fluorescence intensity (MFI) in large populations (5000) of target cells after infection. Previously we reported that REAF affects the production of reverse transcripts early after infection and that at this critical time point REAF is transiently down modulated in HeLa-CD4 (21). Here we confirmed that the loss of REAF from MDMs also occurs early, where the Vpr dependent loss of REAF is observed from 30 minutes after infection (Figure 1I) with recovery around 2 hours. In contrast, without Vpr (HIV-1 89.6$^{\Delta vpr}$) the opposite occurs, REAF levels *increase* after infection. The increase in REAF levels is most potent after 30 mins of infection with HIV-1 89.6$^{\Delta vpr}$.

Previously it was reported that Vpr is released from the capsid and enters the nucleus shortly after infection (11). We generated a virus with a mutated form of Vpr (F34I) described as lacking the ability to localise to the nuclear membrane or to interact with the nuclear transport proteins importin-α and nucleoporins (22). Interestingly, HIV-1 89.6$^{F34I}$, similar to HIV-1 89.6$^{\Delta vpr}$, can no longer deplete REAF in MDMs (Figure 1H). We confirmed that HIV-1 89.6$^{\Delta vpr}$ has restricted replication in MDMs compared with the wild type virus expressing Vpr (HIV-1 89.6$^{WT}$) (Figure 1I). Like HIV-1 89.6$^{\Delta vpr}$, the mutant virus (HIV-1 89.6$^{F34I}$) replicates less efficiently in MDMs.

Other targets of Vpr have been proposed. It recruits SLX4-SLX1/MUS81-EME1 endonucleases to DCAF1, activating MUS81 degradation and triggering arrest in G2/M (23). It

also degrades helicase-like transcription factor (HLTF) (13) and has recently been shown to enhance infection of HIV-1 in T-cells lines (Yan *et al.* 2019). We show here both HLTF (Figure 1J) and MUS81 (Figure 1K) are depleted by virus concurrently with REAF within 60 minutes of infection. In contrast to REAF, HLTF and MUS81 levels do not recover.

**Fluctuation of subcellular REAF expression after HIV-1 infection is Vpr dependent.**

In view of the above, using imaging flow cytometry, we sought to determine the relative subcellular localization of REAF. We found that REAF is mostly present in the nuclear compartment compared to the cytoplasm (Figure 2A) of both Hela-CD4 (left) and particularly so in primary macrophages (right). We looked more carefully at the cellular distribution of REAF at the early time points following HIV-1 infection. Here, HeLa-CD4 infected with HIV-1 $89.6^{WT}$ or HIV-1 $89.6^{\Delta vpr}$ were quantified for REAF nuclear or cytoplasmic protein over the first three hours following infection by imaging flow cytometry. Following challenge with HIV-1 $89.6^{\Delta vpr}$, REAF levels increase in both the nucleus (~25%, Figure 2B, left) and cytoplasm (~10%, Figure 2B, right) within 0.5 hours and nuclear levels remain high for 3 hours. However, in the presence of Vpr (HIV-1 $89.6^{WT}$) the observed increase in REAF is curtailed, with a steady decline from 0.5-2 hours. The decline is most marked in the nucleus with ~20% reduction by 1 hour and ~30% at 2 hours. By 3 hours, levels of REAF protein recover. The virus carries finite quantities of Vpr (17), which potentially explains why there is a pause in the down modulation of REAF. Imaging flow cytometry software determined the 'nuclear enrichment score' over time after infection with HIV-1 $89.6^{WT}$ or HIV-1 $89.6^{\Delta vpr}$ (Figure 2C). The lower the score the less REAF in the nucleus relative to in the cell overall. By 1-2 hours, a significant segregation emerges and so the presence of Vpr, relative nuclear levels of REAF are suppressed. Lower levels of REAF were also observed in the

cytoplasm over time but to a much lesser extent (Figure 2B, right).

Nuclear levels of REAF were compared in a number of primary cell types using imaging flow cytometry (Figure 2D). When compared to either monocytes or resting/activated T cells, both MDMs and dendritic cells (DCs) highly express nuclear REAF. Antiviral factors are often upregulated in response to pathogen associated molecular patterns. Polyriboinosinic:polyribocytidylic acid (poly(I:C)) is a double-stranded RNA, used to stimulate viral infection associated molecular pattern recognition pathways. Figure 2E shows poly(I:C) induction of REAF in THP-1, a macrophage cell line.

We sought to determine if the above fluctuations of REAF observed in HeLa-CD4 cells also occur in MDMs. The subcellular fluctuation of REAF levels from two donors after challenge was determined using imaging flow cytometry. With *vpr* (HIV-1 $89.6^{WT}$), nuclear REAF decreases within 2 hours of viral infection of macrophages from two donors (Figure 2F), similar to that observed in HeLa-CD4 (Figure 2B). In contrast, also in both donors, nuclear REAF rapidly increases from as early as 0.5 hours when the virus does not contain Vpr (HIV-1 $89.6^{\Delta vpr}$) (Figure 2F). For the cytoplasmic compartment, a similar picture emerges for REAF fluctuation. In both donors, when Vpr is absent, REAF levels increase rapidly within 0.5 hours of infection (Figure 2F). This cytoplasmic increase is curtailed in donor 1 when Vpr is present. In donor 2 the loss of Nuclear REAF after HIV-1 $89.6^{WT}$ infection is paralleled by an increase in cytoplasmic REAF. Similar kinetics of *total* REAF protein fluctuation were observed, in the presence or absence of Vpr, in two further donors. This was measured by Western blotting and is presented in Expanded View Figure 1.

We sought to determine if knockdown of REAF in primary macrophages resulted in an increased susceptibility to HIV-1 infection. In Figure 2G primary MDMs were treated with siRNA

targeting REAF (siREAF) or a control protein (siCB). Cells lacking REAF were found to be significantly more susceptible to infection with HIV-1 89.6.

In Figure 2H, MDMs were treated with virus-like particles (VLPs) containing Vpr and Western blotting confirmed that Vpr alone is sufficient to induce the down modulation of REAF. MDMs, pre-treated with VLPs (Figure 2H) were then subsequently infected with either HIV-1 $89.6^{WT}$ or $89.6^{\Delta vpr}$. Cells with VLP-induced down modulation of REAF were found to be significantly more susceptible to infection with either virus but particularly virus lacking Vpr of its own.

**Depletion of REAF results in G2/M accumulation and mitotic cells are more susceptible to HIV-1 infection.**

After knockdown of REAF in THP-1 (THP-1 shRNA-REAF, Figure 3A), there is a clear increase in mitosis, indicated by the phosphorylation of histone H3 (Ser10/Thr11). We further confirmed G2/M arrest after knockdown of REAF in a T cell line, PM1 (PM1-shRNA-REAF, Figure 3B-D). Reduction of REAF mRNA (Figure 3B) and protein (Figure 3C) was confirmed. An accumulation of cells at G2/M, illustrated by the significant increase in G2/G1 ratio (Figure 3D, insert), was seen comparable to previous reports of Vpr induced cell cycle arrest (Figure 3D)(14).

We defined the cell cycle phases (G0/1, S and G2/M) of primary human monocytes and analysed REAF expression. Levels are lowest in G0/1, increase through S phase, and peak in G2/M (Figure 3E). Using imaging flow cytometry, we further analysed the subcellular localization of REAF during mitosis (Figure 3F). An asynchronous population had a nuclear enrichment score of 0.92 (solid grey, left). Nocodazole-treated cells diverged into two populations (0.13, 1.53, Figure

3F, black outline, left). To confirm the divergence in the nuclear enrichment scores corresponded to cell cycle, the mitotic cell marker (histone H3 pSer28) was used to identify such cells. Mitotic cells were shown to have a lower nuclear enrichment score (0.17), and thus lower levels of REAF in the nucleus relative to the cell overall. The treatment of cells with nocodazole resulted in an increase in the population with a low nuclear enrichment score (Figure 3F, right). Representative images are shown in Figure 3G. Using confocal microscopy, REAF is observed in both the cytoplasm and nucleus through interphase, prophase and prometaphase but excluded from chromatin during metaphase, anaphase and telophase (Figure 3H).

Vpr has been shown, to varying degrees, to be more beneficial for replication in macrophages than in cycling T cells *(22, 24-27)*. We compared the susceptibility of a mitotic enriched population of HeLa-CD4 to an asynchronous population (Figure 3I-K). A thymidine/nocodazole treated population was confirmed to be mitotic enriched using flow cytometry (Figure 3I) and Western blotting (Figure 3J). The mitotic enriched population was more susceptible to infection with HIV-1 $89.6^{WT}$ (approximately 7-11 fold, Figure 3K). A further experiment using HIV-1 89.6 (VSV-G) with a GFP reporter as a challenge virus confirmed the increased susceptibility of mitotic cells to infection (Expanded View Figure 2).

IFNα induces many HIV restriction factors (28, 29). We used RNA microarray analysis to determine if IFNα upregulated REAF mRNA in MDMs. Figure 4A shows IFNα induced upregulation of antiviral genes, including HIV restriction factors APOBEC3G, IFITM1-3, MX2, Tetherin and Viperin (30) but with little or no upregulation of REAF mRNA. Nor was REAF mRNA upregulated in MDMs or $CD4^+$ T cells in response to IFNα (Figure 4B).

Restriction factors are often under evolutionary positive selection at sites that interact with virus. We compared REAF DNA sequences from 15 extant primate species using PAML package

for signatures of positive natural selection. We found no evidence of positive selection of REAF in the primate lineage (Figure 4C).

## Discussion

The deletion of *vpr* in HIV-1 leads to significant impairment of replication in both HeLa-CD4 and primary macrophages. A number of experiments presented here point to a role for Vpr in the counter-restriction of the antiviral protein REAF. First, HIV-1 replication is significantly enhanced by knockdown of REAF in either HeLa-CD4 or primary macrophages and this phenotype is even more pronounced for viruses lacking *vpr*. Second, REAF is down modulated early after infection in a manner dependent on both the presence of Vpr and, as demonstrated by a *vpr* single point mutation, its localisation to the nuclear envelope. Third, using VLPs we show that Vpr alone is sufficient to down modulate REAF in MDMs. Finally, we show, by co-immunoprecipitation, that REAF and Vpr physically interact with each other either directly or as part of a complex. Taken together, our results highlight the importance of the relationship between REAF and the HIV-1 accessory protein Vpr.

Others have shown a specific requirement for Vpr in infection of non-dividing cells and only reduced replication rates in cycling T cells (20). Indeed, REAF is more highly expressed MDMs compared to cycling T cells. The requirement for Vpr in macrophage infection is substantiated here where reduced viral particle production is observed after infection of MDMs with either HIV-1 $89.6^{\Delta vpr}$ or HIV-1 $89.6^{F34I}$ compared to HIV-1 $89.6^{WT}$. This is the first demonstration of a *vpr*-alleviated impairment of HIV-1 replication in primary macrophages. Recently however Yan *et al.* (2019) show that HLTF, a proposed target of Vpr, restricts replication

of HIV-1 in T cells while Lahouassa *et al.* (2016) also reported a Vpr dependent loss of HLTF at six hours post infection (8). Our results also support a role for HLTF in HIV replication. We show that HLTF down modulation occurs concomitantly with REAF as early as 0.5 hours post infection. Interestingly, HLTF and REAF were identified in the same screen for proteins that interact with single-stranded DNA (31).

The transient nature and timing of REAF depletion is consistent with its ability to impede the production of reverse transcripts early in infection (21). After an initial down modulation of REAF following infection REAF depletion is paused one hour later, perhaps attributable to the finite quantities of Vpr carried in the virus particle (17). In contrast however, down modulation of HLTF and MUS81 (another proposed target of Vpr) is maintained, perhaps suggesting alternate or additional roles for these factors later in infection (27, 22). Recently, Greenwood *et al.*, using a whole cell proteomics screen for factors up or down modulated by Vpr in T cells, identified HLTF among almost 2000 proteins affected, underlining the promiscuous activity of Vpr (14). It is now critical, in light of these findings, that attention is directed to those proposed Vpr targets that affect replication of HIV-1 in primary cells. The recovery of REAF expression prior to 6 hours after infection most likely explains why it was not identified in the data collected by Greenwood *et al.* (14).

Our model is that Vpr is brought into the cell by HIV-1, in limited, but sufficient quantities to down modulate REAF in the timeframe required for reverse transcription to proceed unhindered. Nuclear localisation of Vpr is required for the down modulation of REAF perhaps similar to the Vpx mediated depletion of the reverse transcription inhibitor SAMHD1, for which degradation is initiated in the nucleus(32). We propose that REAF is linked to the innate immune response as treatment of primary macrophages with poly(I:C) induces its expression. Furthermore, HIV-1

without *vpr*, induces the expression of REAF to high levels in primary macrophages within 0.5 hours of infection.

A poorly understood phenomenon is that Vpr induces cell cycle arrest in the G2/M phase after infection. We report here that the loss of REAF from cycling cells contributes to an accumulation of the population in G2/M. Other studies suggest that *vpr* is less dispensable for infection of non-dividing cells (20). In fact, REAF is more highly expressed MDMs compared to cycling T cells supporting this premise.

REAF is unlike the evolving HIV restriction factors like APOBEC3G, SAMHD1, TRIM5 or BST2/Tetherin and is more similar to SERINC3 and 5 which are not under positive selection (33, 34). We propose that REAF is a multi-functional or 'moonlighting' protein with at least two cellular roles (35). REAF has many properties of restriction factors (30, 36). It interacts with HIV-1 reverse transcripts, impeding reverse transcription (21). It is germline encoded, constitutively expressed in cells, regulated by the proteasome system, suppressed by Vpr and upregulated by poly(I:C). Our results support the current model for Vpr activity which is that it induces the degradation of a protein involved in an unknown restriction of HIV-1.

## Materials and Methods

### Ethics Statement

Leucocyte cones from blood donors, from which PBMCs were isolated, were obtained from the NHS Blood Transfusion service, St. George's Hospital, London. Donors were anonymous and thus patient consent was not required. The local ethical approval reference number is

06/Q0603/59.

**Cell Lines**

HEK-293T (ATCC), PM1, THP-1, C8166, HeLa-CD4 parental (all NIBSC AIDS Reagents) and HeLa-CD4 shRNA-REAF (previously described) were maintained at 37°C in 5% $CO_2$ (18). Cells were cultured in Dulbecco's Modified Eagle Medium (DMEM, ThermoFisher) supplemented with fetal bovine serum (FBS) 5-10% from Thermo Fisher and appropriate antibiotics. HeLa-CD4-shRNA-REAF were selected for resistance to puromycin in media supplemented with 10µg/ml puromycin.

The isopropyl β-D-1-thiogalactopyranoside (IPTG)-inducible vector pLKO-IPTG-3xLacO (Sigma) was used to express short hairpin RNAs (shRNAs) targeted against REAF (Sigma Mission TRCN0000141116). Additionally, a non-target (scramble) control was prepared. Viral particles for cell line transductions were prepared by co-transfecting HEK-293T cells with pLKO-IPTG-3xLacO, the Gag/Pol packaging vector pLP1, a Rev expression vector pLP2, and the vesicular stomatitis virus G protein (VSV-G) expression vector pVPack-VSV-G (Stratagene). After 72 hours, virus was clarified by low-speed centrifugation and passed through a 0.45-m-pore-size filter. THP-1 and PM1 cells were transduced by culturing viral particles in the presence of 8g/ml Polybrene for 72 hours, after which resistant colonies were selected and maintained with 2µg/ml puromycin. Culturing cells in the presence of 1mM IPTG for 72 hours induced expression of shRNAs.

**Transfections and Virus/VLP Production**

The HIV-1 primary isolate 2044 has been previously described (19). The infectious molecular clone for HIV-1 89.6 was obtained from the Centre for AIDS Research (NIBSC, UK). Infectious full-length and chimeric HIV clones were prepared by linear polyethylenimine 25K (Polysciences), Lipofectamine 2000 (Invitrogen) or Lipofectamine 3000 (Invitrogen) transfection of HEK-293T. Virus-like particles (VLPs) were produced by linear polyethylenimine 25K (Polysciences) transfection of HEK-293T. The VLP packaging vector was a gift from N. Landau and production is described in reference (20). HIV-1 89.6 (VSV-G) was generated by combining the transfer vector pCSGW with the envelope pMDG VSV-G and the core construct p8.91-89.6gag in HEK-293T as has been previously described *(21)*.

Plasmid constructs HIV-1 89.6$^{\Delta vif}$, HIV-1 89.6$^{\Delta vpr}$ and HIV-1 89.6$^{\Delta vpu}$ were generated from the HIV-1 89.6 molecular clone, using overlap extension PCR *(29)*. Clones were confirmed by plasmid sequencing (Source BioScience). Primer sequences are available upon request. HIV-1 p89.6 *vpr* mutant F341 was made by site directed mutagenesis (Agilent) of the p89.6 plasmid. HEK-293T were plated at $2x10^4/cm^2$ in 8-well chamber slides (for confocal microscopy), or 10cm dishes (for virus and VLP production) 48 hours prior to transfection. For virus/VLP production, supernatant was harvested 72 hours post transfection and cleared of cell debris by centrifugation at 500 x *g* for 5 minutes. Stocks were stored at -80$^0$C. All viruses were amplified by C8166 for 48 hours before harvest.

**Titration of Replication Competent Virus**

HeLa-CD4 were seeded at $1.5\times10^4$ cells/well in 48-well plates to form an adherent monolayer of cells. Cell monolayers were challenged with serial 1/5 dilutions of virus and titre was assessed after 48 hours by *in situ* intracellular staining of HIV-1 p24 to identify individual

foci of viral replication (FFU), as described previously *(21)*. For infection time course experiments, 400-500µl of $1\times10^5$ FFU/ml (HeLa-CD4) or $3\times10^3$ FFU/ml (MDMs) virus was added per well to cells cultured in 6-well trays for 24 hours (HeLa-CD4) or 7 days (for MDMs). For Figure 3I, cells were challenged with 50ng p24 in 6-well plates with $2\times10^6$ MDMs per well. Supernatants were harvested on days 0, 2, 8, 21 and 28 post challenge and p24 concentration analysed by ELISA.

**p24 ELISA**

ELISA plates were pre-coated with 5µg/ml sheep anti-HIV-1 p24 antibody (Aalto Bio Reagents) at 4°C overnight. Viral supernatants were treated with 1% Empigen® BB for 30 minutes at 56°C, then plated at 1:10 dilution in Tris-bufered saline (TBS) on anti-p24-coated plates and incubated for 3 hours at room temperature. Alkaline phosphatase-conjugated mouse anti-HIV-1 p24 monoclonal antibody (Aalto Bio Reagents) diluted in 20% sheep serum, 0.05% v/v Tween-20, TBS was then added and incubated for 1 hour at room temperature. Plates were washed 4 times with 0.01% v/v Tween-20 in PBS and twice with ELISA Light washing buffer (ThermoFisher). CSPD substrate with Sapphire II enhancer (ThermoFisher) was added and incubated for 30 minutes at room temperature before a plate reader was used to detect chemiluminiscence.

**cDNA Synthesis and qPCR**

Total RNA was extracted from PM1 cells using the ReliaPrep RNA kit (Promega) and in one-step reverse transcription qPCR (Quantbio) using TaqMan probes for the detection of amplified transcripts. Data acquisition was performed on an Agilent Mx3000 and analyzed on MxPro software.

From MDMs, total RNA was extracted using an RNeasy Plant Mini Kit (QIAGEN), and

cDNA was synthesized with SuperScript™ III First-Strand Synthesis System (Invitrogen), according to manufacturer's instructions. cDNA was subjected to real-time quantitative PCR (qPCR) using REAF, OAS1 and β-actin primer pairs with SYBR® Green detection of amplified transcripts (QuantiTect SYBR Green PCR Kit, QIAGEN). Data acquisition and analysis were performed using the ABI PRISM™ 7500 SDS software. Primer sequences are available upon request.

**Gene Expression RNA Microarray**

Prior to microarray analysis, RNA from MDMs was prepared using the Illumina™ TotalPrep™ RNA Amplification Kit (Ambion), according to manufacturer's instructions. The probes were hybridized on an Illumina™ HT12v3 bead array following the manufacturer's standard hybridization and scanning protocols. Raw measurements were processed by GenomeStudio software (Illumina), and quantile normalized. All microarray data are publicly available in the Gene Expression Omnibus (GEO) database with accession number GSE54455.

**IFN, Poly(I:C) and Treatment**

MDMs, $CD4^+$ T cells and THP-1 were treated with IFN (100-500IU/ml, specified) for 24 or 48 hours (specified) before harvest for RNA extraction; analysis by Western blotting or imaging flow cytometry. THP-1 were treated with poly(I:C) (25μg/ml, HMW/LyoVec™, Invitrogen) for 48 hours before analysis by Western blotting or imaging flow cytometry. Prior to IFN or poly(I:C) treatment, THP-1 were treated with phorbol 12-myristate 13-acetate (PMA, 62ng/ml) for 3 days and then PMA-free DMEM for 2 days to allow differentiation and recovery. For Figure 4A and Figure S6C-D, recombinant IFNα was purchased from Sigma (Interferon-αA/D human Cat. No.

I4401-100KU) and is a combination of human subtypes 1 and 2. For Figure S6A-B and E, recombinant human IFNs are from Peprotech.

**Western blotting**

Cells were harvested and lysed in 30-50µl of radioimmunoprecipitation assay (RIPA) buffer supplemented with NaF (5µM), $Na_2VO_3$ (5µM), β-glycerophosphate (5µM) and 1x Protease Inhibitor Cocktail (Cytoskeleton). The protein concentration of each sample was determined using BCA Protein Assay Kit (Pierce). 12.5-70µg of total protein was separated by SDS-PAGE (4-12% Bis-Tris Gels, Invitrogen), at 120V for 1 hour 45 minutes in MOPS SDS Running Buffer (Invitrogen). Separated proteins were transferred onto nitrocellulose membrane (0.45µm pore size, GE Healthcare) at 45V for 2 hours, in ice-cold 20% (v/v) Methanol NuPAGE™ Transfer Buffer (ThermoFisher). Membranes were blocked for 1 hour at room temperature in 5% (w/v) non-fat milk powder in TBS-T buffer. Specific proteins were detected with primary antibodies by incubation with membranes overnight at $4^0$C and with secondary antibodies for 1 hour at room temperature. All antibodies were diluted in blocking buffer. Proteins were visualized using ECL Prime Western Blotting Detection Reagent (GE Healthcare) and imaged using either ChemiDoc Gel Imaging System (Bio-Rad) or exposed to CL-XPosure films (ThermoScientific) and developed.

**Antibodies**

Primary rabbit polyclonal antibody to REAF (RbpAb-RPRD2) has been previously described (21). For imaging flow cytometry and confocal microscopy, RbpAb-RPRD2 was detected using goat anti-rabbit IgG conjugated with Alexa Fluor 647 (Invitrogen). FITC-labelled

anti-phospho-histone H3 (Ser28) Alexa 488 was used (BD Bioscience) for imaging flow cytometry and confocal microscopy. MsmAb-IFITM1 (clone 5B5E2, Proteintech), was detected by goat anti-mouse IgG Alexa Fluor 555 (ThermoFisher) for imaging flow cytometry, and by anti-mouse IgG antibody conjugated to HRP (GE Healthcare) for Western blotting, as were MsmAb-Mus81 and MsmAb-GFP (both Abcam). Also for Western blotting, RbpAb-RPRD2, RbmAb-IFITM3 (EPR5242, Insight Biotechnology), RbpAb-GAPDH, RbpAb-βActin, RbmAb-phospho-histone H3 (Ser10/Thr11) and RbpAb-HLTF (all Abcam) were detected with secondary antibody: donkey anti-rabbit IgG conjugated to HRP (GE Healthcare).

**Immunoprecipitation**

HEK-293T, transfected with either VPR-GFP or GFP control expression vector, were lysed 72hrs post transfection in RIPA buffer supplemented with NaF (5µM), $Na_2VO_3$ (5µM), β-glycerophosphate (5µM) and 1x Protease Inhibitor Cocktail (Cytoskeleton). Total protein concentration was determined using BCA Protein Assay Kit (Pierce). GFP-TRAP® magnetic agarose beads were equilibrated in ice cold dilution buffer (10 mM Tris/Cl pH 7.5; 150 mM NaCl; 0.5 mM EDTA) according to manufacturer's instructions (Chromotek). Cell lysates containing 100µg of total protein were incubated with 10µl of equilibrated beads for 2 hours at 4$^0$C with gentle agitation. Beads were washed three times with PBST buffer before analysis by Western blotting.

**Magnetic Separation of Primary Human Lymphocytes**

Peripheral blood mononuclear cells (PBMCs) were isolated from leukocyte cones (NHS Blood Transfusion service, St. George's Hospital, London) by density gradient centrifugation with

Lymphoprep™ density gradient medium (STEMCELL™ Technologies). Peripheral monocytes were isolated from PBMCs, using the human $CD14^+$ magnetic beads (Miltenyi Biotech) according to manufacturer's instructions. $CD4^+$ T cells were isolated from the flow-through, using the human $CD4^+$ T cell isolation kit (Miltenyi Biotech). $CD14^+$ monocytes, and $CD4^+$ T cells were either differentiated, or fixed directly after isolation for intracellular staining. To obtain M1 and M2 macrophages (M1/M2 MDMs), monocytes were treated with either granulocyte-macrophage colony stimulating factor (GM-CSF, 100ng/ml, Peprotech) or macrophage colony stimulating factor (M-CSF, 100ng/ml) for 7 days, with medium replenished on day 4. To obtain dendritic cells (DC), monocytes were treated with GM-CSF (50ng/ml) and IL-4 (50ng/ml) for 7 days, with medium replenished on day 4. Activated $CD4^+$ T cells were obtained by stimulating freshly isolated $CD4^+$ T cells at $1x10^6$/ml with T cell activator CD3/CD28 Dynabeads (ThermoFisher), at a bead-cell-ratio of 1, for 7 days. Magnetic beads were removed prior to intracellular staining and flow cytometry.

**Immunofluorescence**

Transfected cells were washed with PBS and fixed in 2% paraformaldehyde/PBS for 10 minutes, at room temperature. Fixed cells were then permeabilized in 0.2% Triton™-X100/PBS for 20 minutes, at room temperature. Cells were incubated with primary antibodies in PBS containing 0.1% Triton-X100 and 2% BSA overnight at $4^0$C. After 3 washes in PBS, cells were then labeled with secondary antibodies in the same buffer for 1 hour, at room temperature, and washed 3 times with PBS. For confocal microscopy, nuclei were counterstained with Hoechst 33342 (2µM, ThermoFisher) for 5 minutes, at room temperature. Labeled cells were mounted with ProLong™ Diamond Antifade Mountant (ThermoFisher) and analyzed on a laser scanning

confocal microscope LSM 710 (Carl Zeiss). Images were acquired with ZEN software and analyzed with ImageJ.

**Imaging Flow Cytometry**

Cells were fixed in FIX&PERM® Solution A (Nordic MUbio) for 30 minutes, and permeabilized with 0.2% Triton™-X 100/PBS. MDMs were blocked with human serum (1%). The staining buffer used was: 0.1% Triton™-X 100 0.5% FBS. Nuclei were stained with DAPI (1µg/ml) for two hours. Imaging flow cytometry was performed using the Amnis ImageStream®x Mark II Flow Cytometer (Merck) and INSPIRE® software (Amnis). A minimum of 10,000 events were collected for each sample, gating strategy is shown in Figure S7. IDEAS® software (Amnis) was used for analysis and to determine the 'nuclear enrichment score'. The nuclear enrichment score is a comparison of the intensity of REAF fluorescence inside the nucleus to the total fluorescence intensity of the entire cell. A lower nuclear enrichment score indicates a lower proportion of overall REAF is located within the nucleus.

**Statistics**

Statistical significance in all experiments was calculated by Student's t-test (two tailed) or ANOVA (indicated). Data are represented as mean ± standard deviation (error bars). GraphPad Prism and Excel were used for calculation and illustration of graphs.

**Cells Synchronization**

HeLa-CD4 were synchronized at the G2/M border by nocodazole (200ng/ml) for 16 hours. Where synchronized cells were infected with virus, an initial S phase block with thymidine (4mM)

was induced for 24 hours followed by a PBS wash and a treatment with nocodazole (100ng/ml) for a further 16 hours. Collecting only those cells that were in suspension, as well as those that detached easily with a manual "shake-off", enriched the population of mitotic cells.

**Cell Cycle Analysis**

Cell cycle phase distribution was determined by analysis of DNA content via either flow cytometry (BD FACS Canto™ II) or imaging flow cytometry. Cells were fixed in ice-cold ethanol (70%), treated with ribonuclease A (100µg/ml) and stained with propidium iodide (PI, 50µg/ml) or fixed in FIX&PERM® Solution A (Nordic MUbio) and stained with DAPI (1µg/ml). Mitotic cells were also identified by flow cytometry using the anti-phospho-histone H3 (Ser28) antibody. Cell lysates were assessed by Western blotting using the anti-phospho-histone H3 (Ser10/Thr11) antibody as an additional mitotic marker. Chromatin morphology and anti-phospho-histone H3 (Ser28) were used to determine the cells in indicated phases of the cell cycle and mitosis in confocal microscopy experiments. Cell cycle status of PM1 cells was determined via propidium iodide (PI) staining using FxCycle PI/RNse solution (ThermoFisher). Stained cells were analyzed on an NxT flow cytometer (ThermoFisher).

**Evolutionary Analysis**

To ascertain the evolutionary trajectory of REAF, we analyzed DNA sequence alignments of REAF from 15 species of extant primates using codeml (as implemented by PAML 4.2) (37). The evolution of REAF was compared to several NSsites models of selection, M1, M7 and M8a (neutral models with site classes of dN/dS <1 or ≤1) and M2, M8 (positive selection models allowing an additional site class with dN/dS >1). Two models of codon frequencies (F61 and F3x4)

and two different seed values for dN/dS (ω) were used in the maximum likelihood simulations. Likelihood ratio tests were performed to evaluate which model of evolution the data fit significantly better. The p-value indicates the confidence with which the null model (M1, M7, M8a) can be rejected in favor of the model of positive selection (M2, M8). The alignment of REAF was analyzed by GARD to confirm the lack recombination during REAF evolution (38). Neither positively selected sites nor signatures of episodic diversifying selection were detected within REAF by additional evolutionary analysis by REL and FEL or MEME (39).

**Data Availability**

All RNA microarray data is available in the gene expression omnibus (GEO) database with accession number GSE54455.

## References:


1. **Eckstein DA, Sherman MP, Penn ML, Chin PS, De Noronha CM, Greene WC, Goldsmith MA.** 2001. HIV-1 Vpr enhances viral burden by facilitating infection of tissue macrophages but not nondividing CD4+ T cells. J Exp Med **194:**1407-1419.
2. **Malim MH, Emerman M.** 2008. HIV-1 accessory proteins--ensuring viral survival in a hostile environment. Cell Host Microbe **3:**388-398.
3. **Zhou X, DeLucia M, Ahn J.** 2016. SLX4-SLX1 Protein-independent Down-regulation of MUS81-EME1 Protein by HIV-1 Viral Protein R (Vpr). J Biol Chem **291:**16936-16947.
4. **Schrofelbauer B, Yu Q, Zeitlin SG, Landau NR.** 2005. Human immunodeficiency virus type 1 Vpr induces the degradation of the UNG and SMUG uracil-DNA glycosylases. J Virol **79:**10978-10987.
5. **Romani B, Shaykh Baygloo N, Aghasadeghi MR, Allahbakhshi E.** 2015. HIV-1 Vpr Protein Enhances Proteasomal Degradation of MCM10 DNA Replication Factor through the Cul4-DDB1[VprBP] E3 Ubiquitin Ligase to Induce G2/M Cell Cycle Arrest. J Biol Chem **290:**17380-17389.
6. **Maudet C, Sourisce A, Dragin L, Lahouassa H, Rain JC, Bouaziz S.** 2013. HIV-1 Vpr induces the degradation of ZIP and sZIP, adaptors of the NuRD chromatin remodeling complex, by hijacking DCAF1/VprBP. PLoS ONE **8**.
7. **Lv L, Wang Q, Xu Y, Tsao LC, Nakagawa T, Guo H, Su L, Xiong Y.** 2018. Vpr Targets TET2 for Degradation by CRL4(VprBP) E3 Ligase to Sustain IL-6 Expression and Enhance HIV-1 Replication. Mol Cell **70:**961-970 e965.
8. **Lahouassa H, Blondot ML, Chauveau L, Chougui G, Morel M, Leduc M.** 2016. HIV-1 Vpr degrades the HLTF DNA translocase in T cells and macrophages. Proc Natl Acad Sci USA **113**.
9. **Laguette N, Brégnard C, Hue P, Basbous J, Yatim A, Larroque M.** 2014. Premature activation of the SLX4 complex by Vpr promotes G2/M arrest and escape from innate immune sensing. Cell **156**.
10. **Hrecka K, Hao C, Shun MC, Kaur S, Swanson SK, Florens L, Washburn MP, Skowronski J.** 2016. HIV-1 and HIV-2 exhibit divergent interactions with HLTF and UNG2 DNA repair proteins. Proc Natl Acad Sci U S A **113:**E3921-3930.
11. **Hofmann S, Dehn S, Businger R, Bolduan S, Schneider M, Debyser Z, Brack-Werner R, Schindler M.** 2017. Dual role of the chromatin-binding factor PHF13 in the pre- and post-integration phases of HIV-1 replication. Open Biol **7**.
12. **Yan J, Shun MC, Zhang Y, Hao C, Skowronski J.** 2019. HIV-1 Vpr counteracts HLTF-mediated restriction of HIV-1 infection in T cells. Proc Natl Acad Sci U S A **116:**9568-9577.
13. **Lahouassa H, Blondot ML, Chauveau L, Chougui G, Morel M, Leduc M, Guillonneau F, Ramirez BC, Schwartz O, Margottin-Goguet F.** 2016. HIV-1 Vpr degrades the HLTF DNA translocase in T cells and macrophages. Proc Natl Acad Sci U S A **113:**5311-5316.
14. **Greenwood EJD, Williamson JC, Sienkiewicz A, Naamati A, Matheson NJ, Lehner PJ.** 2019. Promiscuous Targeting of Cellular Proteins by Vpr Drives Systems-Level Proteomic Remodeling in HIV-1 Infection. Cell Rep **27:**1579-1596 e1577.

15. **Cohen EA, Terwilliger EF, Jalinoos Y, Proulx J, Sodroski JG, Haseltine WA.** 1990. Identification of HIV-1 vpr product and function. J Acquir Immune Defic Syndr **3:**11-18.
16. **Bachand F, Yao XJ, Hrimech M, Rougeau N, Cohen EA.** 1999. Incorporation of Vpr into human immunodeficiency virus type 1 requires a direct interaction with the p6 domain of the p55 gag precursor. J Biol Chem **274:**9083-9091.
17. **Desai TM, Marin M, Sood C, Shi J, Nawaz F, Aiken C, Melikyan GB.** 2015. Fluorescent protein-tagged Vpr dissociates from HIV-1 core after viral fusion and rapidly enters the cell nucleus. Retrovirology **12:**88.
18. **Marno KM, O'Sullivan E, Jones CE, Diaz-Delfin J, Pardieu C, Sloan RD, McKnight A.** 2017. RNA-Associated Early-Stage Antiviral Factor Is a Major Component of Lv2 Restriction. J Virol **91**.
19. **Simmons G, Reeves JD, McKnight A, Dejucq N, Hibbitts S, Power CA, Aarons E, Schols D, De Clercq E, Proudfoot AE, Clapham PR.** 1998. CXCR4 as a functional coreceptor for human immunodeficiency virus type 1 infection of primary macrophages. J Virol **72:**8453-8457.
20. **Connor RI, Chen BK, Choe S, Landau NR.** 1995. Vpr is required for efficient replication of human immunodeficiency virus type-1 in mononuclear phagocytes. Virology **206**.
21. **Marno KM, Ogunkolade BW, Pade C, Oliveira NM, O'Sullivan E, McKnight A.** 2014. Novel restriction factor RNA-associated early-stage anti-viral factor (REAF) inhibits human and simian immunodeficiency viruses. Retrovirology **11:**3.
22. **Vodicka MA, Koepp DM, Silver PA, Emerman M.** 1998. HIV-1 Vpr interacts with the nuclear transport pathway to promote macrophage infection. Genes Dev **12:**175-185.
23. **Laguette N, Bregnard C, Hue P, Basbous J, Yatim A, Larroque M, Kirchhoff F, Constantinou A, Sobhian B, Benkirane M.** 2014. Premature activation of the SLX4 complex by Vpr promotes G2/M arrest and escape from innate immune sensing. Cell **156:**134-145.
24. **Connor RI, Chen BK, Choe S, Landau NR.** 1995. Vpr is required for efficient replication of human immunodeficiency virus type-1 in mononuclear phagocytes. Virology **206:**935-944.
25. **Heinzinger NK, Bukrinsky MI, Haggerty SA, Ragland AM, Kewalramani V, Lee MA, Gendelman HE, Ratner L, Stevenson M, Emerman M.** 1994. The Vpr protein of human immunodeficiency virus type 1 influences nuclear localization of viral nucleic acids in nondividing host cells. Proc Natl Acad Sci U S A **91:**7311-7315.
26. **Balliet JW, Kolson DL, Eiger G, Kim FM, McGann KA, Srinivasan A.** 1994. Distinct effects in primary macrophages and lymphocytes of the human immunodeficiency virus type 1 accessory genes vpr, vpu, and nef: mutational analysis of a primary HIV-1 isolate. Virology **200**.
27. **Chen R, Le Rouzic E, Kearney JA, Mansky LM, Benichou S.** 2004. Vpr-mediated incorporation of UNG2 into HIV-1 particles is required to modulate the virus mutation rate and for replication in macrophages. J Biol Chem **279:**28419-28425.
28. **Goujon C, Malim MH.** 2010. Characterization of the alpha interferon-induced postentry block to HIV-1 infection in primary human macrophages and T cells. J Virol **84:**9254-9266.

29. **Cheney KM, McKnight A.** 2010. Interferon-alpha mediates restriction of human immunodeficiency virus type-1 replication in primary human macrophages at an early stage of replication. PLoS One **5:**e13521.
30. **Doyle T, Goujon C, Malim MH.** 2015. HIV-1 and interferons: who's interfering with whom? Nat Rev Microbiol **13:**403-413.
31. **Marechal A, Li JM, Ji XY, Wu CS, Yazinski SA, Nguyen HD, Liu S, Jimenez AE, Jin J, Zou L.** 2014. PRP19 transforms into a sensor of RPA-ssDNA after DNA damage and drives ATR activation via a ubiquitin-mediated circuitry. Mol Cell **53:**235-246.
32. **Brandariz-Nunez A, Valle-Casuso JC, White TE, Laguette N, Benkirane M, Brojatsch J, Diaz-Griffero F.** 2012. Role of SAMHD1 nuclear localization in restriction of HIV-1 and SIVmac. Retrovirology **9:**49.
33. **McLaren PJ, Gawanbacht A, Pyndiah N, Krapp C, Hotter D, Kluge SF, Gotz N, Heilmann J, Mack K, Sauter D, Thompson D, Perreaud J, Rausell A, Munoz M, Ciuffi A, Kirchhoff F, Telenti A.** 2015. Identification of potential HIV restriction factors by combining evolutionary genomic signatures with functional analyses. Retrovirology **12:**41.
34. **Murrell B, Vollbrecht T, Guatelli J, Wertheim JO.** 2016. The Evolutionary Histories of Antiretroviral Proteins SERINC3 and SERINC5 Do Not Support an Evolutionary Arms Race in Primates. J Virol **90:**8085-8089.
35. **Jeffery CJ.** 2014. An introduction to protein moonlighting. Biochem Soc Trans **42:**1679-1683.
36. **Kluge SF, Sauter D, Kirchhoff F.** 2015. SnapShot: antiviral restriction factors. Cell **163:**774-774 e771.
37. **Yang Z.** 2007. PAML 4: phylogenetic analysis by maximum likelihood. Mol Biol Evol **24:**1586-1591.
38. **Kosakovsky Pond SL, Posada D, Gravenor MB, Woelk CH, Frost SD.** 2006. GARD: a genetic algorithm for recombination detection. Bioinformatics **22:**3096-3098.
39. **Pond SL, Frost SD.** 2005. Datamonkey: rapid detection of selective pressure on individual sites of codon alignments. Bioinformatics **21:**2531-2533.

**Acknowledgements:** This work was supported partly by an MRC Senior Non-Clinical Fellowship awarded to AM (G117/547) and PhD studentships awarded by QMUL Life Sciences Institute (LSI) (CEJ) and The Rosetrees Trust (JMG and CEJ, M665 and M275). RDS was supported by the Wellcome Trust-University of Edinburgh Institutional Strategic Support Fund. The monoclonal antibodies to HIV-1 p24 (EVA365 and 366) were provided by the EU Programme EVA Centre for AIDS Reagents, NIBSC, UK (AVIP Contract Number LSHP-CT-2004-503487). The Wellcome Trust (101604/Z/13/Z) funded the purchase of Amnis ImageStream™ imaging flow cytometer. We wish to thank N. Landau for the kind gift of VPL constructs.

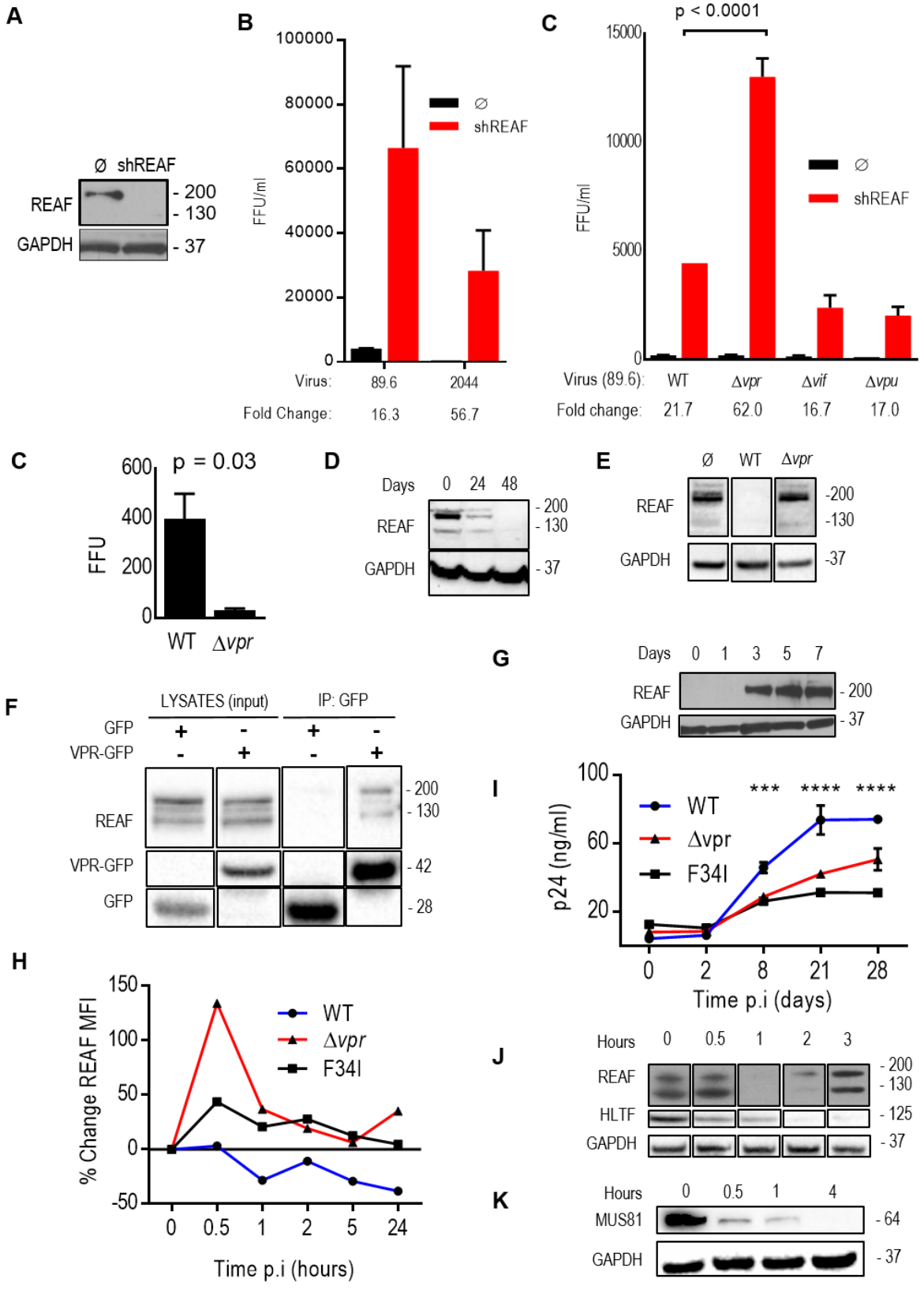


610

**Figure 1: HIV-1 Vpr interacts with REAF and overcomes restriction. (A)** Infectivity (FFU/ml) of HIV-1 89.6, NL4.3 and 2044 in HeLa-CD4 (Ø) and HeLa-CD4 shRNA-REAF (shREAF). **(B)** HeLa-CD4 shRNA-REAF (shREAF) challenged with HIV-1 $89.6^{WT}$ or mutants HIV-1 $89.6^{\Delta vpr}$, $^{\Delta vif}$ or $^{\Delta vpu}$. HIV-1 $89.6^{\Delta vpr}$ are >40 fold more sensitive to REAF restriction than HIV-1 $89.6^{WT}$ or other mutants. Viral inputs were equivalent at approximately 50 FFU/ml measured on HeLa-CD4. Error bars indicate the standard deviations of means derived from a range of duplicate titrations. INSERT: REAF protein in HeLa-CD4 (Ø) and HeLa-CD4 shRNA-REAF (shREAF). GAPDH is a loading control. **(C)** Resulting FFU from equal p24 inputs (1ng) of HIV-1 $89.6^{WT}$ or HIV-1 $89.6^{\Delta vpr}$ in HeLa-CD4. **(D)** REAF protein in PM1 at indicated times (hours) post challenge with HIV-1 $89.6^{WT}$. GAPDH is a loading control. **(E)** REAF protein in Hela-CD4 24 hours post challenge with HIV-1 $89.6^{WT}$ or HIV-1 $89.6^{\Delta vpr}$. GAPDH is a loading control. **(F)** 293T cells were transfected with Vpr-GFP or GFP control plasmid and protein was immunoprecipitated (IP) with anti-GFP beads. Co-immunoprecipitated REAF was detected in the Vpr-GFP precipitation. **(G)** REAF protein during monocyte to macrophage differentiation at indicated days with M-CSF treatment. GAPDH is a loading control. **(H)** Imaging flow cytometry of total REAF protein in MDMs over time post challenge with HIV-1 $89.6^{WT}$, HIV-1 $89.6^{\Delta vpr}$ or HIV-1 $89.6^{F34I}$. **(I)** Infectivity of HIV-1 $89.6^{WT}$ compared with HIV-1 $89.6^{\Delta vpr}$ and HIV-1 $89.6^{F34I}$ in MDMs. p24 antigen concentrations over 28 days post infection are indicated. Viral input was equivalent at 50ng of p24. Error bars represent standard deviations of means of duplicates (*** = $P < 0.001$; **** = $P < 0.0001$, two-way ANOVA; the same results were obtained for HIV-1 $89.6^{WT}$ versus HIV-1 $89.6^{\Delta vpr}$ and HIV-1 $89.6^{F34I}$). Data is representative of at least two independent experiments. **(J)** REAF and HLTF protein in THP-1 over time post challenge with HIV-1 $89.6^{WT}$.

GAPDH is a loading control. **(K)** MUS81 protein in Hela-CD4 over time post challenge with HIV-1 89.1$^{WT}$. GAPDH is a loading control.

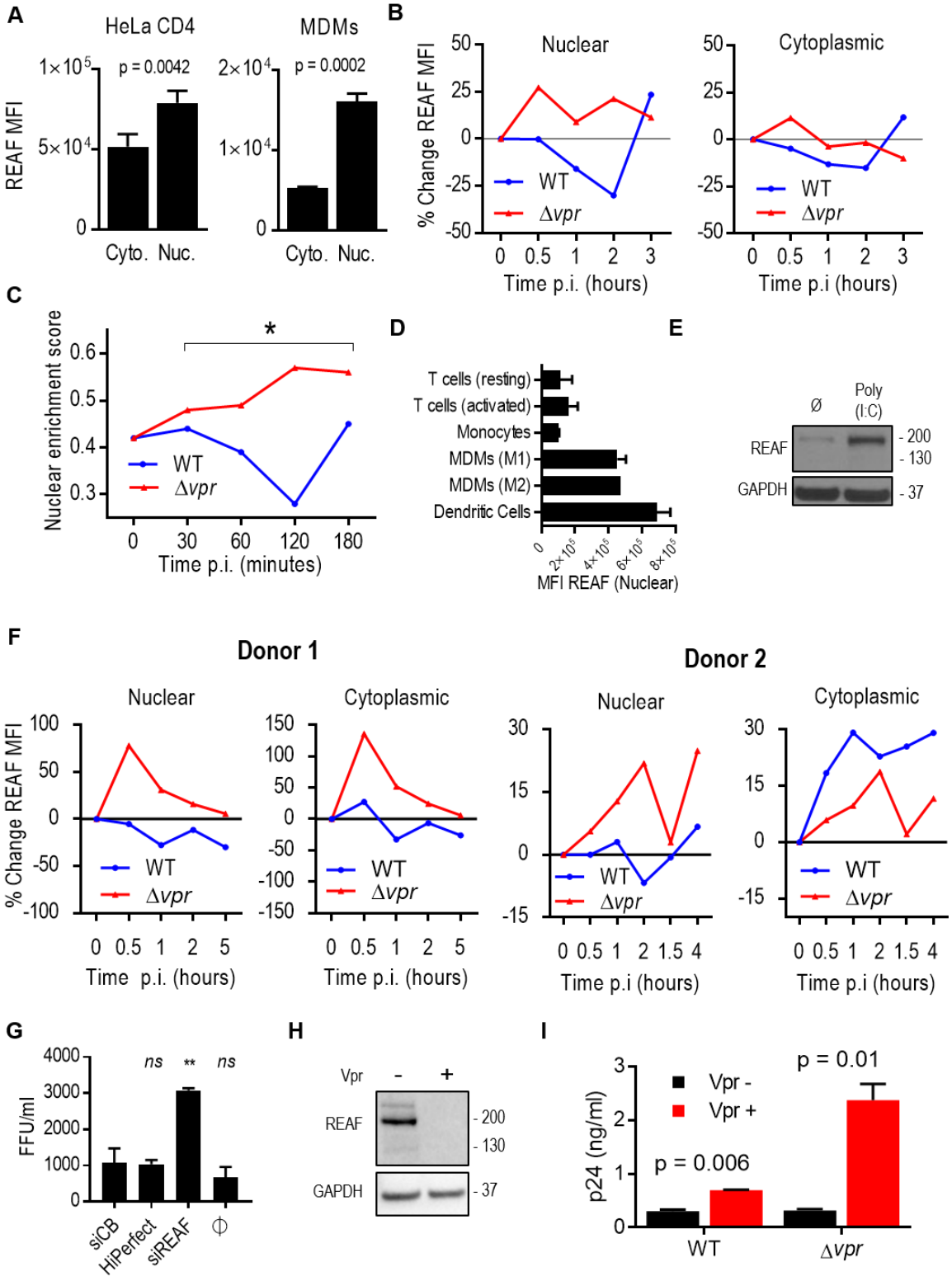

**Figure 2: Fluctuation of subcellular REAF expression after HIV-1 infection is Vpr dependent. (A)** Nuclear and cytoplasmic REAF mean fluorescence intensity (MFI) in HeLa-CD4 (left) and MDMs (right) measured by imaging flow cytometry. Error bars represent standard deviations of means of replicates. **(B)** Percentage (%) change in REAF MFI in the nucleus (left) and cytoplasm (right) of Hela-CD4 over time after challenge with HIV-1 $89.6^{WT}$ or HIV-1 $89.6^{\Delta vpr}$. Results are representative of three independent experiments. **(C)** Nuclear enrichment score of HeLa-CD4 over time post challenge with HIV-1 $89.6^{WT}$ or HIV-1 $89.6^{\Delta vpr}$. A lower nuclear enrichment score indicates a lower proportion of overall REAF is located in the nucleus as calculated by IDEAS software. Results are representative of three independent experiments. **(D)** Nuclear REAF MFI in indicated primary cell types measured by imaging flow cytometry. Error bars represent standard deviations of means of two donors. **(E)** REAF protein in PMA differentiated THP-1 after poly(I:C) treatment. GAPDH is a loading control. **(F)** Percentage (%) change in subcellular REAF MFI in MDMs over time after challenge with HIV-1 $89.6^{WT}$ or HIV-1 $89.6^{\Delta vpr}$ measured by imaging flow cytometry. Data from two donors are presented. **(G)** Infectivity (FFU/ml) of HIV-1 $89.6^{WT}$ in MDMs transfected with siRNA-REAF. HiPerfect (transfection reagent) and siCB are negative controls. ** = $P<0.01$, *ns* = not significant, one-way ANOVA and *post hoc* Dunnett's test. **(H)** REAF protein in MDMs treated with empty or Vpr-containing VLPs. GAPDH is a loading control. VLP input was equivalent at 100ng of p24. **(I)** Viral particle production (p24 concentration) in MDMs pre-treated with VLPs (H) measured at 20 days post challenge with HIV-1 $89.6^{WT}$ or HIV-1 $89.6^{\Delta vpr}$.

681

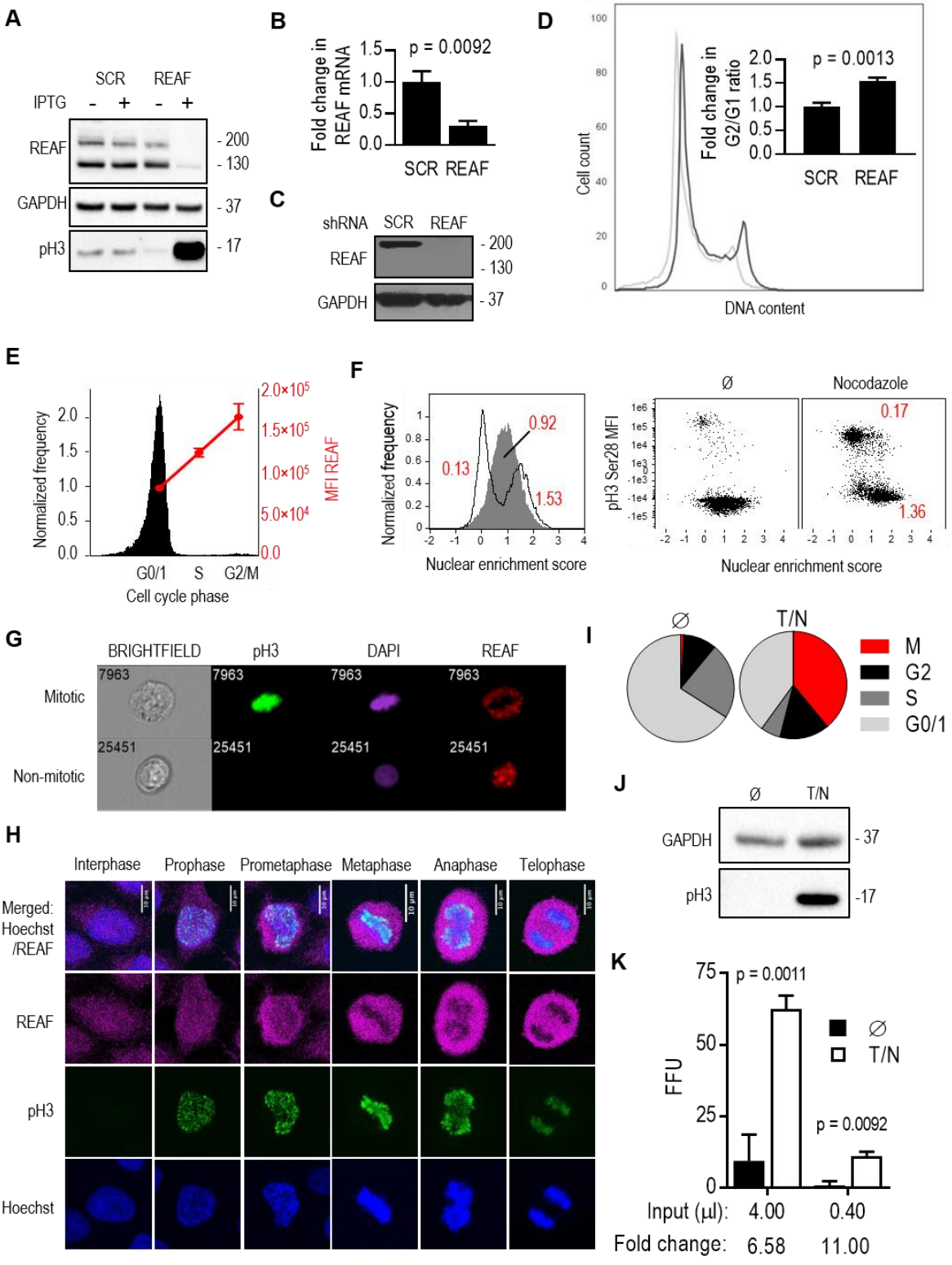


682

683 **Figure 3: Depletion of REAF results in G2/M accumulation and mitotic cells are more**
684 **susceptible to HIV-1 infection. (A)** REAF protein in THP-1 with IPTG-inducible shRNA
685 targeting REAF (shREAF) or a scrambled control sequence (shSCR). Phospho-histone H3
686 (Ser10/Thr11) is a mitotic marker and GAPDH is a loading control. (**B)** Fold change in mRNA
687 transcript level in PM1 shREAF normalized to PM1 shSCR measured by qPCR **(C)** REAF protein
688 in PM1 expressing shRNA targeting REAF (shREAF) and PM1 expressing a scrambled control
689 sequence (shSCR). GAPDH is a loading control. **(D)** Flow cytometry of cell cycle phase in PI
690 stained PM1 shREAF (black outline) and PM1 shSCR (grey outline). Plot shown is representative
691 of three biological replicates. Insert shows fold change in G2/G1 ratio in PM1 shREAF normalized
692 to PM1 shSCR. Error bars represent standard deviations of means of three biological replicates.
693 **(E)** Imaging flow cytometry of cell cycle phase and REAF protein in DAPI stained primary
694 monocytes **(F-G)** Imaging flow cytometry of subcellular REAF in nocodazole treated HeLa-CD4.
695 A lower nuclear enrichment score indicates a lower proportion of overall REAF in the nucleus -
696 untreated: 0.92, nocodazole-treated: 0.13 (one population), 1.53 (another population) (left).
697 Phospho-histone H3 (Ser28) staining confirmed mitotic cells had a lower score of 0.17 (right).
698 Representative images (G) of subcellular REAF in mitotic and non-mitotic cells. **(H)** Confocal
699 microscopy of subcellular REAF in HeLa-CD4. Phospho-histone H3 (Ser28) staining and
700 chromatin morphology (Hoechst) were used for cell cycle phase identification. **(I)** Flow cytometry
701 was used to determine cell cycle profiles (pie charts) of DAPI and phospho-histone H3 (Ser28)
702 stained HeLa-CD4 (Ø) and cells synchronized at the G2/M border (T/N) by thymidine/nocodazole
703 treatment. **(J)** Western blotting confirmed an enriched population of mitotic cells in the
704 synchronized population using phospho-histone H3 (Ser10/Thr11) as an alternative mitotic cell
705 marker and GAPDH as a loading control. **(K)** Cells in (I) were challenged with HIV-1 $89.6^{WT}$.

706 Viral infectivity was assessed 48 hours post challenge by intracellular staining of HIV-1 p24 to
707 identify focus-forming units (FFUs). Viral input and fold change in infectivity are indicated.
708
709
710
711
712
713
714
715
716
717
718
719
720
721
722
723
724
725
726
727

728

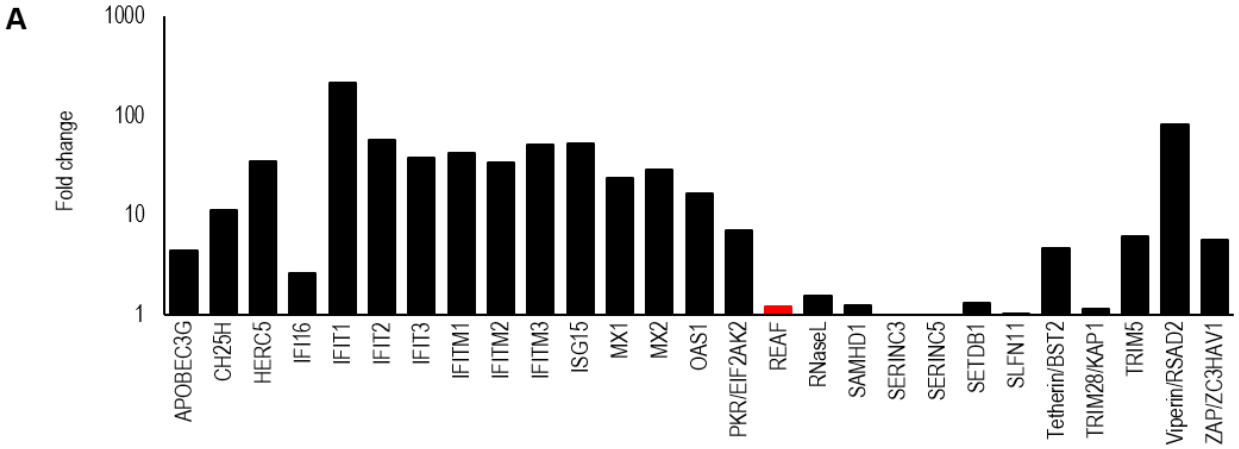


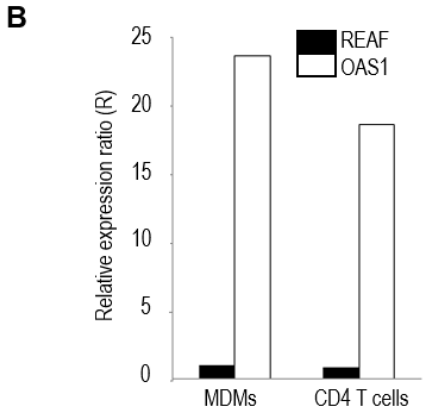


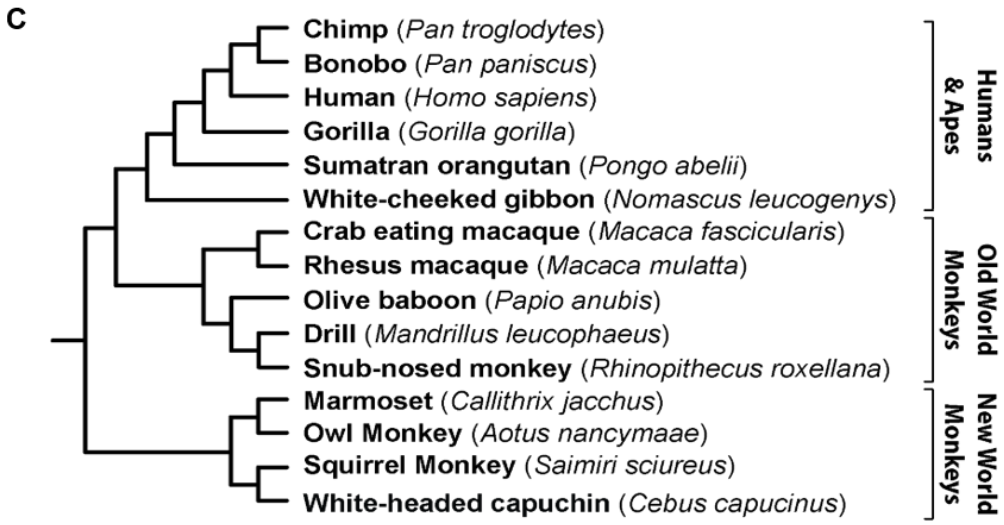


| | | M1 vs M2 | | M7 vs M8 | | M8a vs M8 | |
|---|---|---|---|---|---|---|---|
| Codon freq. model | $\omega_o$ | 2*ΔlnL | p-value | 2*ΔlnL | p-value | 2*ΔlnL | p-value |
| Fcodon | 0.4 | 0.67 | 0.72 | 0.95 | 0.62 | 0.67 | 0.41 |
| Fcodon | 1.2 | 0.67 | 0.72 | 0.95 | 0.62 | 0.67 | 0.41 |
| F3x4 | 0.4 | 0.53 | 0.86 | 0.53 | 0.77 | 0.32 | 0.57 |
| F3x4 | 1.2 | 0.53 | 0.86 | 0.53 | 0.77 | 0.32 | 0.57 |

729 **Figure 4: REAF is not IFN stimulated or under positive selection. (A)** RNA-Seq determined
730 change in REAF mRNA compared to other antiviral factors in MDMs treated with IFNα
731 (500IU/ml). **(B)** MDMs and primary $CD4^+$ T cells were treated with IFNα (500IU/ml) for 48 hours.
732 Increase in REAF mRNA, relative to that of β-actin, was measured by qPCR and OAS1 was used
733 as a positive control for IFN induced upregulation **(C)** REAF DNA sequences from 15 extant
734 primate species (tree length of 0.2 substitutions per site along all branches of the phylogeny) (top)
735 were analyzed using the PAML package for signatures of positive natural selection (bottom).
736 Initial seed values for ω ($\omega_O$) and different codon frequency models were used in the maximum
737 likelihood simulation. Twice the difference in the natural logs of the likelihoods (2*InL) of the
738 two models were calculated and evaluated using the chi-squared critical value. The p value
739 indicates the confidence with which the null model (M1, M7, M8a) can be rejected in favor of the
740 model of positive selection (M2, M8).
741
742
743
744
745
746
747
748
749
750
751

**EV Figure 1**

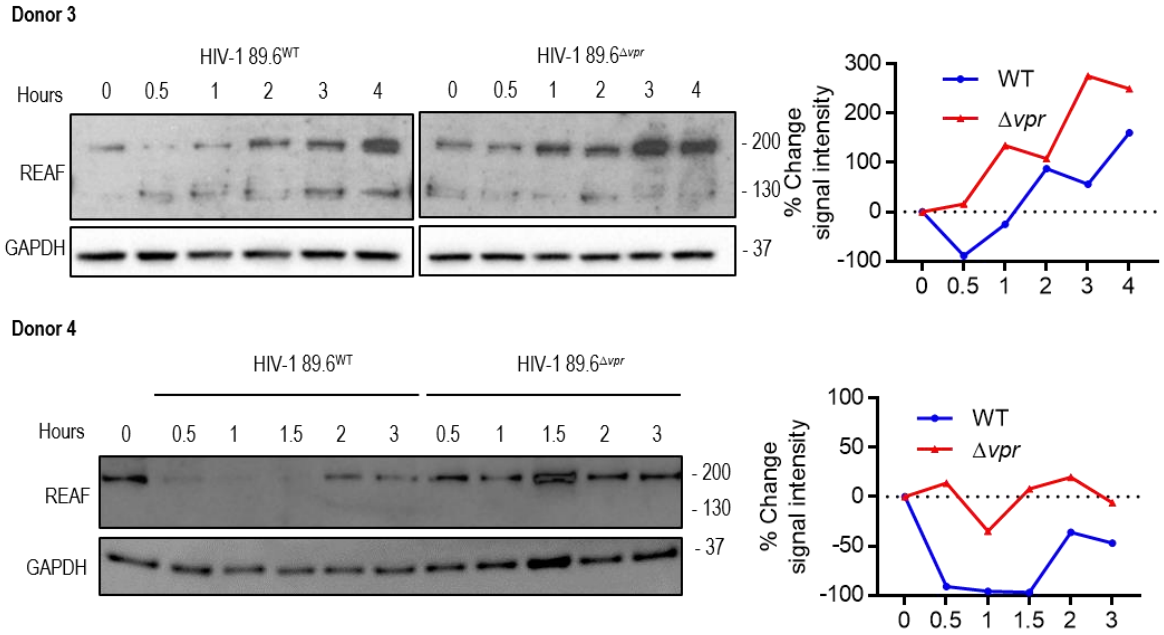


**Expanded View Figure 1: Vpr mediated down modulation of REAF.** REAF protein in MDMs from a further two independent donors over time post challenge with HIV-1 89.6$^{WT}$ or HIV-1 89.6$^{\Delta vpr}$. GAPDH is a loading control. Densitometry of 200kDa REAF relative to GAPDH is presented (right).

764 **EV Figure 2**

765

766 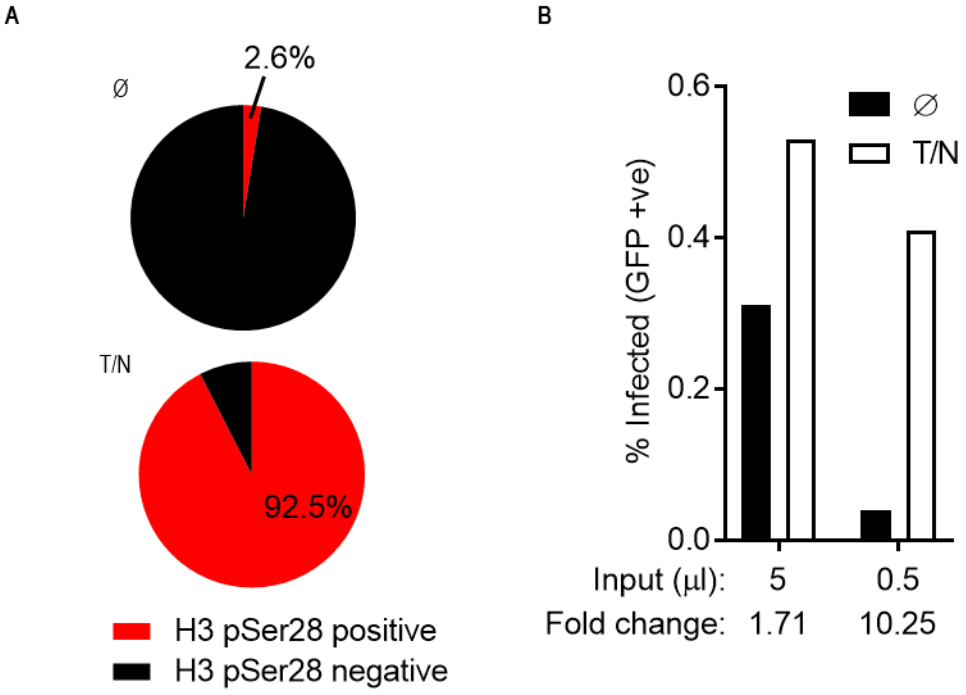


774

775 **Expanded View Figure 2: Mitotic cells are more susceptible to HIV-1 infection. (A)** Flow
776 cytometry of HeLa-CD4 was used to confirm mitotic arrest (92.5%) after thymidine/nocodazole
777 (T/N) treatment (pie charts), phospho-histone H3 (Ser28) is a mitotic cell marker. **(B)** Cells in (A)
778 were challenged with HIV-1 89.6 (VSV-G) with a GFP reporter gene. Viral infectivity was
779 assessed 48 hours after challenge by flow cytometry. Viral input and fold change in infectivity are
780 indicated. This virus does not express Vpr.

781

782

783

784

785

## EV Figure 3

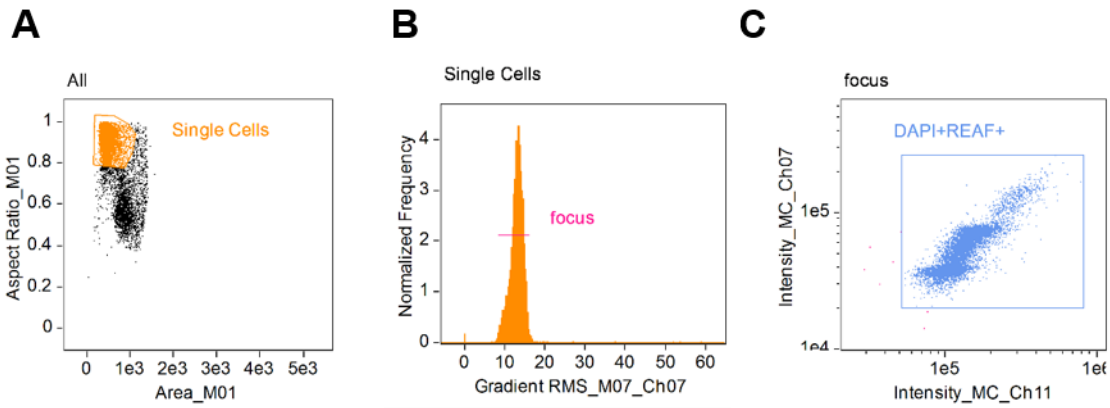


**Expanded View Figure 3: Sequential gating strategy used in imaging flow cytometry analysis with IDEAS software.** For compensation prior to analysis: cells remained unstained for REAF but stained for i) DAPI, ii) FITC-labelled anti-phospho-histone H3 (Ser28) Alexa 488 or (iii) anti-rabbit IgG conjugated with Alexa Fluor 647. **(A)** Single uniformly shaped cells were gated by area versus aspect ratio of the brightfield cell images to exclude doublets (the minor axis of the cell divided by the major axis and is calculated by IDEAS software). **(B)** The small proportion of cell images which were not in focus were excluded from the analysis by using gradient RMS (root mean square of the rate of change of the image intensity profile) to gate and extrapolate quality fluorescence data. **(C)** From single in focus cells, DAPI and REAF positive cells (DAPI+REAF+) were gated for analysis. Representative plot examples are shown.